



Scattering of S^2 kinks

Adalto R. Gomes (UFMA)

Fabiano C. Simas (UFMA)

ArXiv: 2410.10445 [hep-th]



Summary

- Introduction
- Nonlinear $O(3)$ σ model in $(1, 1)$ dimensions
- Geometric and direct coupling
- An extended sine-Gordon model with internal structure
- Scattering results
- Conclusion

Introduction

- Topological defects are field theory solutions with localized density energy that propagate freely without losing form.
- Topological map between the physical coordinate space and the internal field space.
- In (1,1) dimensions, we have the kink and antikink as the simplest topological defects.
- In high dimensionality, one can consider a multiplet multiple of fields with a geometric constraint, as done, for instance, in the nonlinear $O(3)$ sigma model.
- When coupled to gravity, the nonlinear $O(3)$ sigma model gives hairy black holes (C. Herdeiro, I. Perapechka, E. Radu, Ya. Shnir, Gravitating solitons and black holes with synchronised hair in the four dimensional $O(3)$ sigma-model, J. High Energ. Phys. 2019, 111(2019)).

- In (2,1) dimensions, after spontaneous breaking symmetry, every finite energy field configuration corresponds to a mapping $S^2 \rightarrow S^2$. Unstable lump solutions, but their interactions were investigated (W. J. Zakrzewski, Nonlinearity 1991)
- In (1,1) dimensions, after explicit breaking symmetry, every finite energy field configuration corresponds to a mapping $S^1 \rightarrow S^2$ (Yu. Loginov, Phys. Atom. Nuclei 2011). Non-contractible loops in internal space.
- A massive nonlinear $O(3)$ sigma model in (1,1)-dimensions with quadratic potential (A. Alonso-Izquierdo, M. A. Gonzalez Leon, J. Mateos Guilarte, Phys. Rev. Lett. 2008, Phys. Rev. D 2009)
- An interesting aspect of these works is the use of spherical coordinates for the fields, leading to a curved metric for the configuration space. Here the metric components depend on the fields, meaning that there is a geometric constraint.

- Bubble universe collisions (Pontus Ahlqvist, Kate Eckerle and Brian Greene, Kink Collisions in Curved Field Space, J. High Energ. Phys. 2015, 59 (2015))
- Bubbles constraining eternal inflation (Matthew C. Johnson, Carroll L. Wainwright, Anthony Aguirre, Hiranya V. Peiris, Simulating the universe(s) III: observables for the full bubble collision spacetime, JCAP 07, 020 (2016))
- Deformations of sigma models in the plane R^2 and in the sphere S^2 , as well as the transference of solutions between these two manifolds (A. Alonso-Izquierdo, A. J. Balseyro Sebastian, M. A. Gonzalez Leon, Transference of kinks between S^2 and R^2 Sigma models [hep-th/2410.01344]).

Nonlinear $O(3)$ σ model in (1, 1) dimensions

$$S = \int dt dx \left[\frac{1}{2} \partial_\mu \vec{\varphi} \cdot \partial^\mu \vec{\varphi} - \nu(1 - \vec{\varphi} \cdot \vec{\varphi}) \right]$$

$$\vec{\varphi} = (\varphi^1, \varphi^2, \varphi^3)$$

$$\varphi^1 = \sin \chi \cos \phi$$

$$\varphi^2 = \sin \chi \sin \phi$$

$$\varphi^3 = \cos \chi$$

$$S = \int dt dx \left(\frac{1}{2} \partial_\mu \chi \partial^\mu \chi + \frac{1}{2} \sin^2 \chi \partial_\mu \phi \partial^\mu \phi \right)$$

Two coupled real scalar fields (ϕ, χ) in an S^2 internal space

$$g_{ij} = \begin{pmatrix} 1 & 0 \\ 0 & \sin^2 \chi \end{pmatrix}$$

Geometric and direct coupling

$$S = \int dt dx \left(\frac{1}{2} \partial_\mu \chi \partial^\mu \chi + \frac{1}{2} \sin^2 \chi \partial_\mu \phi \partial^\mu \phi - V(\phi, \chi) \right).$$

$$\begin{aligned} \partial_\mu (\sin^2 \chi \partial^\mu \phi) + V_\phi(\phi, \chi) &= 0, \\ \partial_\mu \partial^\mu \chi - \frac{1}{2} \sin(2\chi) \partial_\mu \phi \partial^\mu \phi + V_\chi(\phi, \chi) &= 0 \end{aligned}$$

Static solutions are solutions of the equations

$$\begin{aligned} \frac{d^2 \chi}{dx^2} - \frac{1}{2} \sin(2\chi) \left(\frac{d\phi}{dx} \right)^2 &= V_\chi(\phi, \chi), \\ \frac{d}{dx} \left(\sin^2 \chi \frac{d\phi}{dx} \right) &= V_\phi(\phi, \chi) \end{aligned}$$

BPS method

$$\rho = \frac{1}{2} \sin^2 \chi \left(\frac{d\phi}{dx} \right)^2 + \frac{1}{2} \left(\frac{d\chi}{dx} \right)^2 + V(\phi, \chi).$$

$$V(\phi, \chi) = \frac{1}{2} \frac{W_\phi^2}{\sin^2 \chi} + \frac{1}{2} W_\chi^2.$$

$$\rho = \frac{1}{2} \sin^2 \chi \left(\frac{d\phi}{dx} \mp \frac{W_\phi}{\sin^2 \chi} \right)^2 + \frac{1}{2} \left(\frac{d\chi}{dx} \mp W_\chi \right)^2 + W_\phi \frac{d\phi}{dx} + W_\chi \frac{d\chi}{dx}.$$

$$\frac{d\phi}{dx} = \pm \frac{W_\phi}{\sin^2 \chi}$$

$$\frac{d\chi}{dx} = \pm W_\chi$$

BPS equations

Stability analysis

$$\begin{pmatrix} \tilde{\phi}(x, t) \\ \tilde{\chi}(x, t) \end{pmatrix} = \begin{pmatrix} \phi(x) \\ \chi(x) \end{pmatrix} + a \cos(\omega t) \begin{pmatrix} \eta_1(x) \\ \eta_2(x) \end{pmatrix}$$

$$\hat{\mathcal{H}} \begin{pmatrix} \eta_1 \\ \eta_2 \end{pmatrix} = \begin{pmatrix} \sin(\chi)^2 \omega^2 \eta_1 \\ \omega^2 \eta_2 \end{pmatrix} \quad \hat{\mathcal{H}} = \begin{pmatrix} H_{11} & H_{12} \\ H_{21} & H_{22} \end{pmatrix}$$

$$H_{11} = -\sin(2\chi) \frac{d\chi}{dx} \frac{d}{dx} - \sin^2(\chi) \frac{d^2}{dx^2} + V_{\phi\phi}$$

$$H_{12} = -\sin(2\chi) \frac{d\phi}{dx} \frac{d}{dx} - 2 \cos(2\chi) \frac{d\phi}{dx} \frac{d\chi}{dx} + V_{\phi\chi}$$

$$H_{21} = \sin(2\chi) \frac{d\phi}{dx} \frac{d}{dx} + V_{\chi\phi}$$

$$H_{22} = -\frac{d^2}{dx^2} + \cos(2\chi) \left(\frac{d\phi}{dx} \right)^2 + V_{\chi\chi}$$

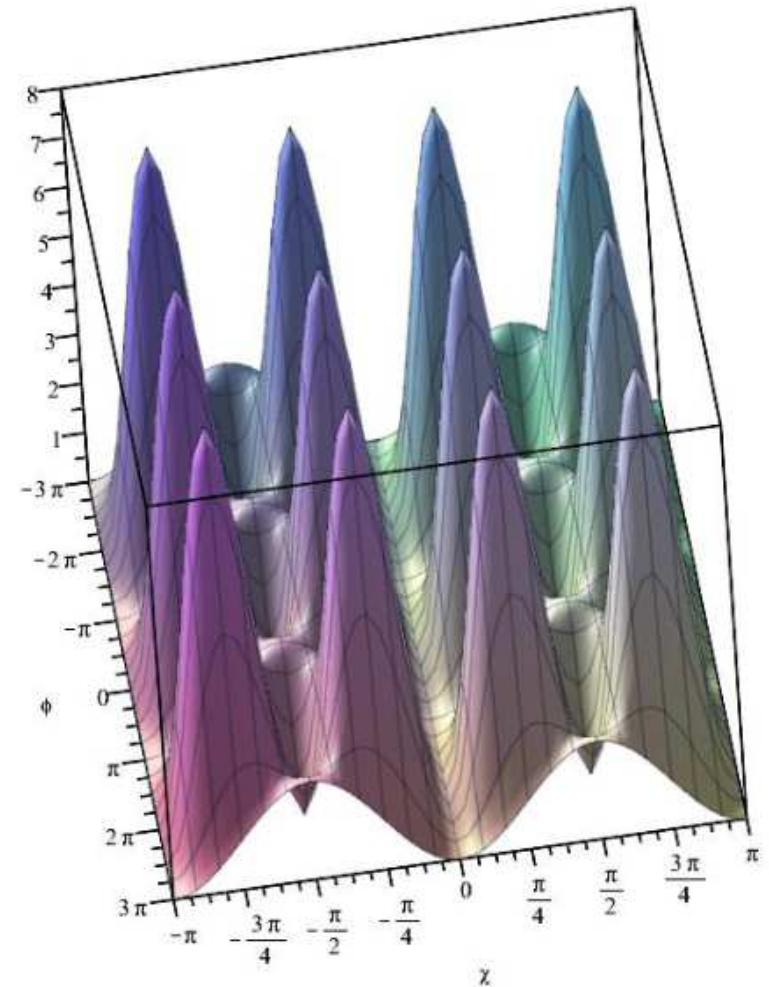
An extended sine-Gordon

$$W_\phi = 2 \sin\left(\frac{\phi}{2}\right) \sin^2 \chi.$$

$$V(\phi, \chi) = 2 \sin^2 \chi \left(\sin^2\left(\frac{\phi}{2}\right) + 16 \cos^2 \chi \cos^2\left(\frac{\phi}{2}\right) \right)$$

$$\phi = \pm 2n\pi, \quad \chi = \pm(2n + 1)\pi/2$$

$$\text{For } S^2: \quad 0 \leq \chi \leq \pi$$



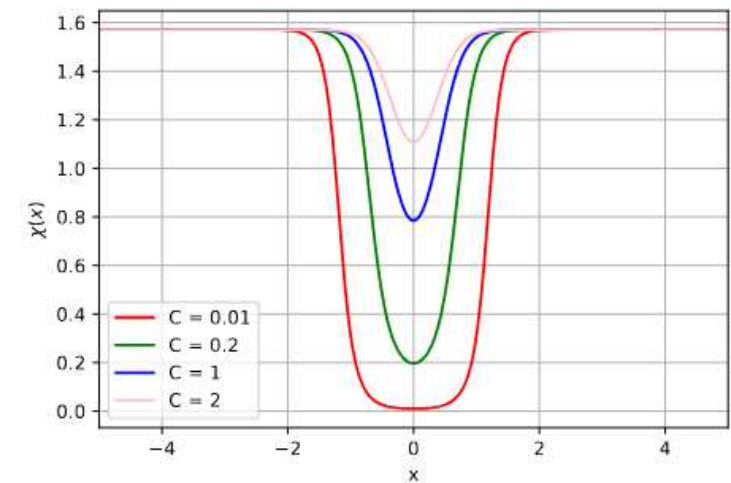
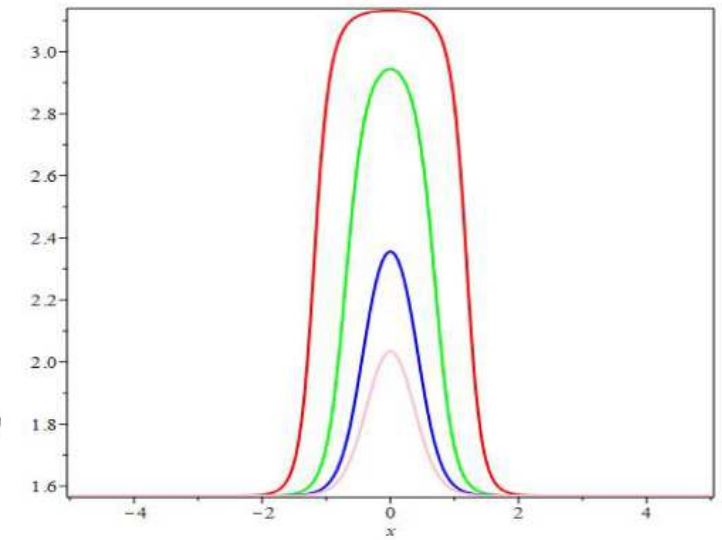
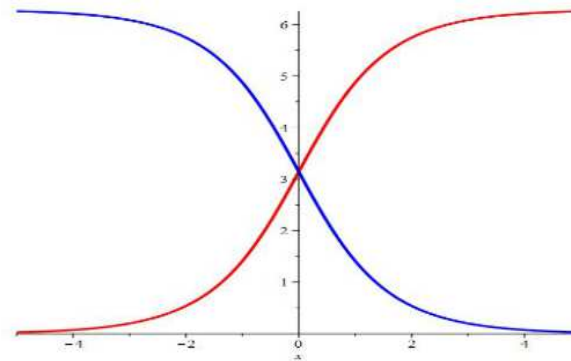
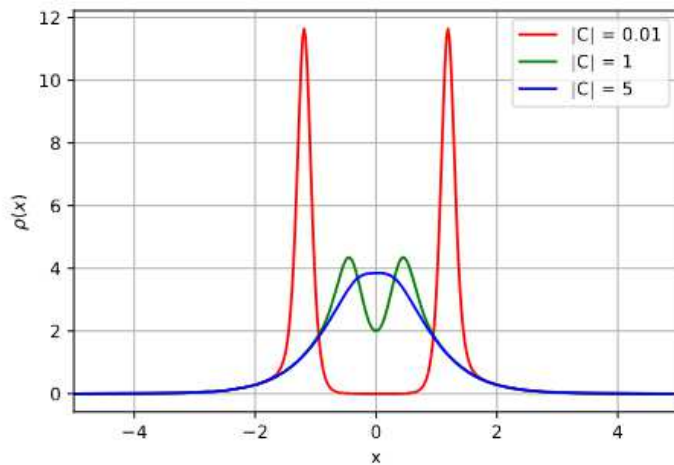
BPS equations and solutions

$$\frac{d\phi}{dx} = \pm 2 \sin\left(\frac{\phi}{2}\right),$$

$$\phi(x) = 4 \arctan(e^x).$$

$$\frac{d\chi}{dx} = \mp 4 \sin(2\chi) \cos\left(\frac{\phi}{2}\right),$$

$$\chi(C, x) = \arctan(C \cosh^8(x)),$$



Soliton solutions in internal space

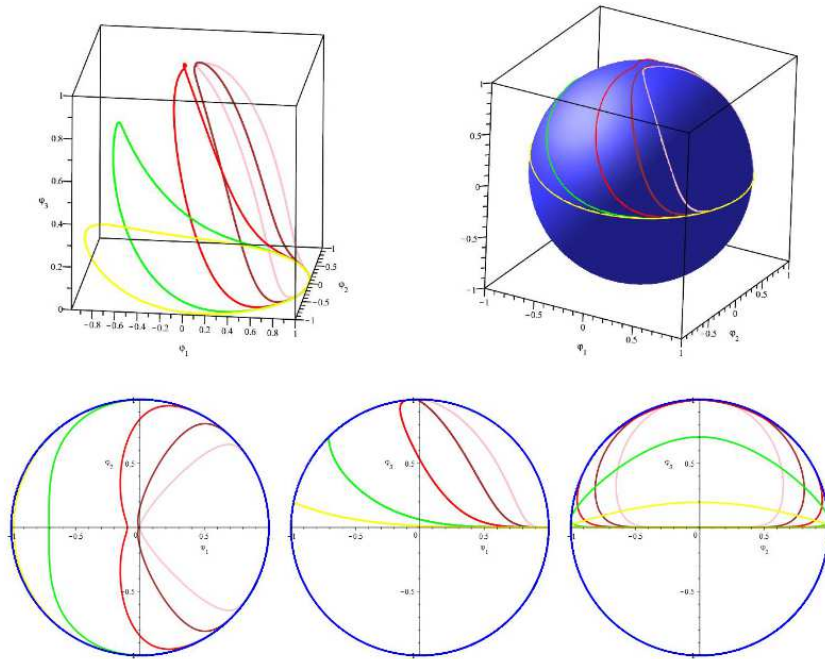


FIG. 4: Soliton solutions in internal space for $C = 10^{-3}$ (pink), $C = 10^{-2}$ (brown), $C = 0.1$ (red), $C = 1$ (green) and $C = 5$ (yellow) a) the soliton solutions are loops in internal space. b) The soliton loops viewed in the S_{int}^2 internal space. c) solitons in phase space $\varphi_1 \times \varphi_2$. d) c) solitons in phase space $\varphi_1 \times \varphi_3$. e) solitons in phase space $\varphi_2 \times \varphi_3$.

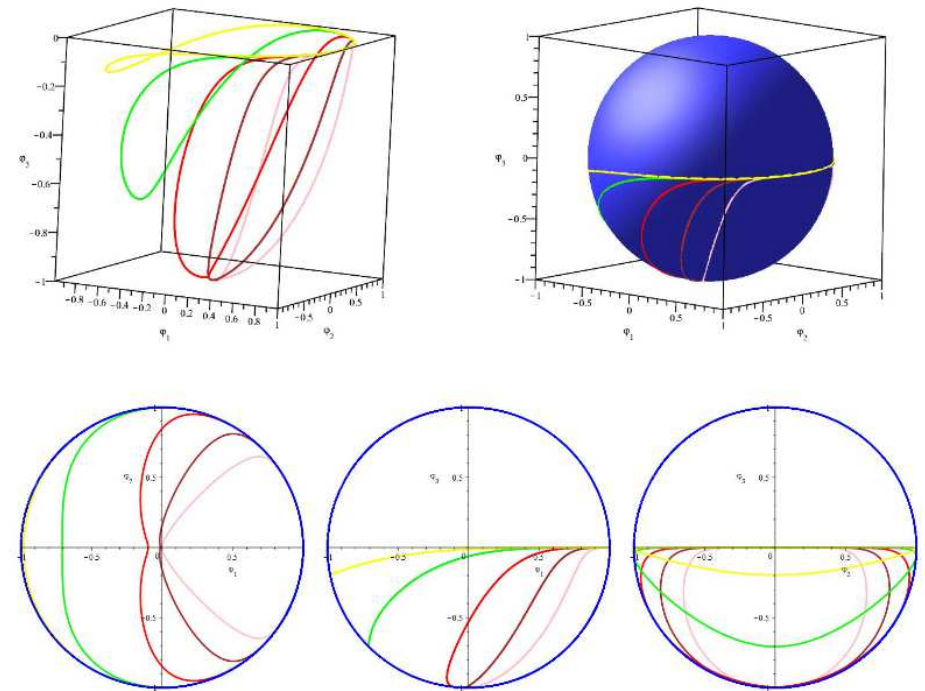


FIG. 5: Soliton solutions in internal space for $C = -10^{-3}$ (pink), $C = -10^{-2}$ (brown), $C = -0.1$ (red), $C = -1$ (green) and $C = -5$ (yellow) a) the soliton solutions are loops in internal space. b) The soliton loops viewed in the S_{int}^2 internal space. c) solitons in phase space $\varphi_1 \times \varphi_2$. d) c) solitons in phase space $\varphi_1 \times \varphi_3$. e) solitons in phase space $\varphi_2 \times \varphi_3$.

Kink-antikink and antilump-antilump scattering

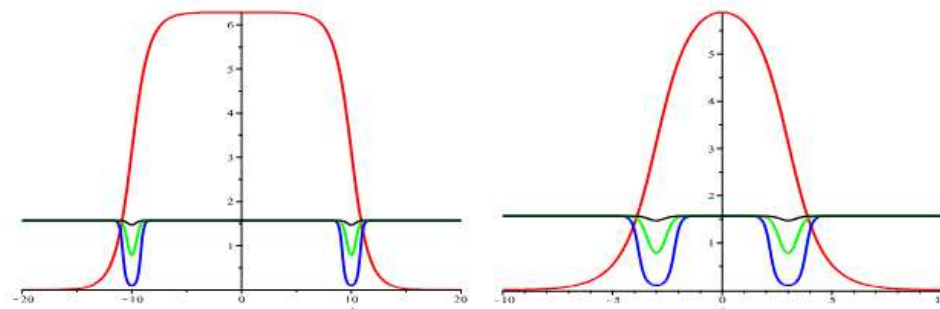


FIG. 7: Initial field configuration for a pair of defects for a) $x_0 = 10$ and b) $x_0 = 3$. For all figures, $\phi(x, t)$ (red) and $\chi(x)$ for $C = 0.1$ (blue), $C = 1$ (green) and $C = 10$ (black).

$$\chi(x, 0, x_0, v) = \chi_K(\gamma(x + x_0 - vt)) + \chi_{\bar{K}}(\gamma(x - x_0 + vt)) - 1,$$

$$\dot{\chi}(x, 0, x_0, v) = \dot{\chi}_K(\gamma(x + x_0 - vt)) + \dot{\chi}_{\bar{K}}(\gamma(x - x_0 + vt)),$$

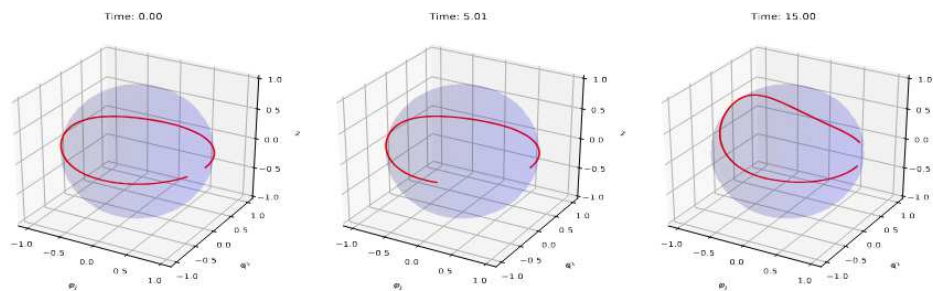
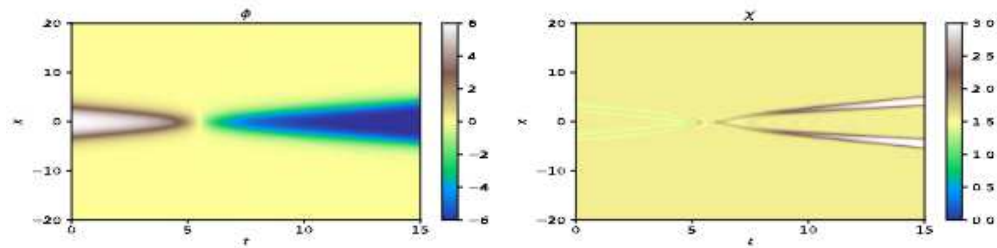
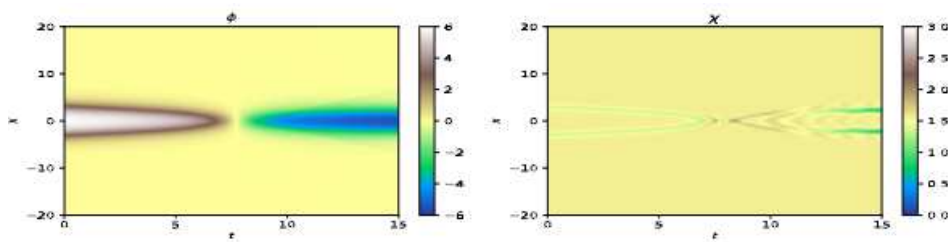
$$\phi(x, 0, x_0, v) = \phi_K(\gamma(x + x_0 - vt)) + \phi_{\bar{K}}(\gamma(x - x_0 + vt)) - \pi,$$

$$\dot{\phi}(x, 0, x_0, v) = \dot{\phi}_K(\gamma(x + x_0 - vt)) + \dot{\phi}_{\bar{K}}(\gamma(x - x_0 + vt)),$$

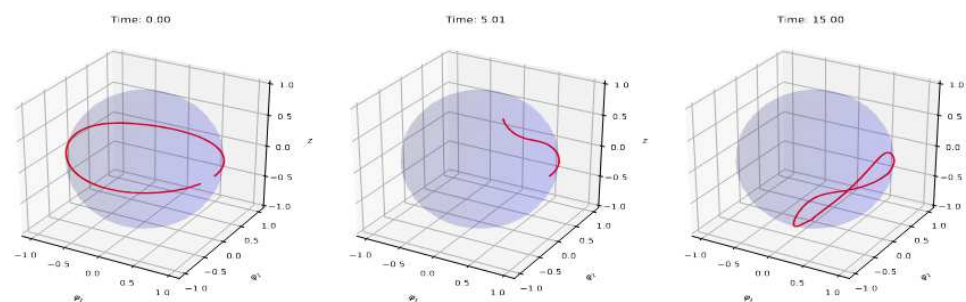
Kink-antikink and antilump-antilump scattering

$v = 0.2, C = 5$

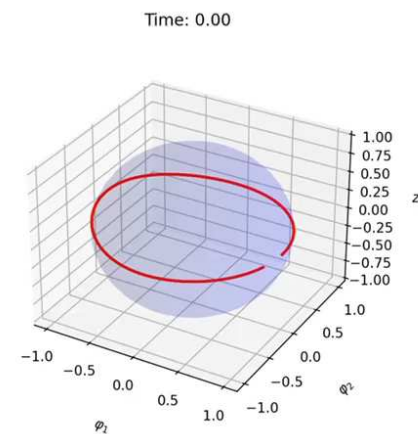
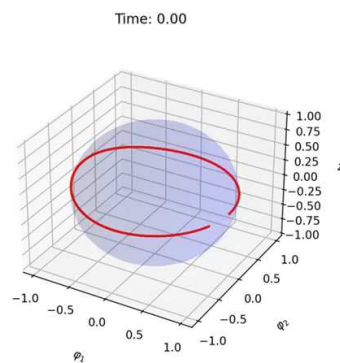
$v = 0.4, C = 5$



(a)



Time: 0.00 Time: 5.01 Time: 15.00



Kink-antikink and lump-antilump scattering

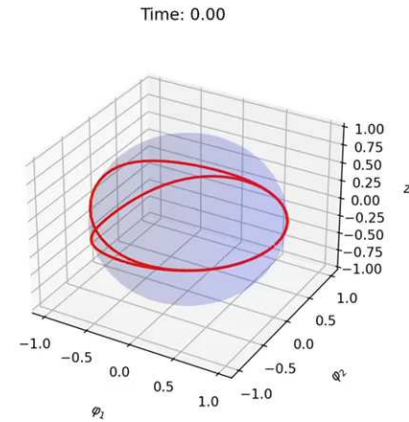
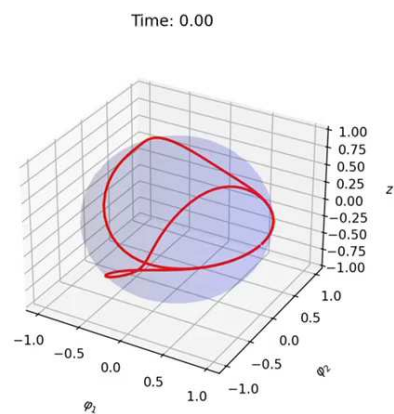
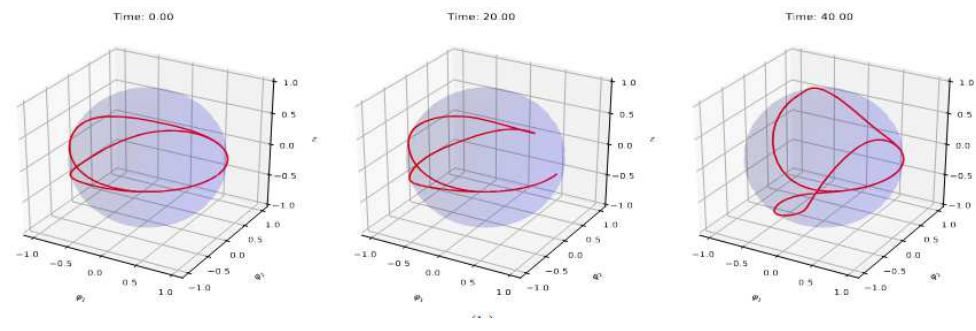
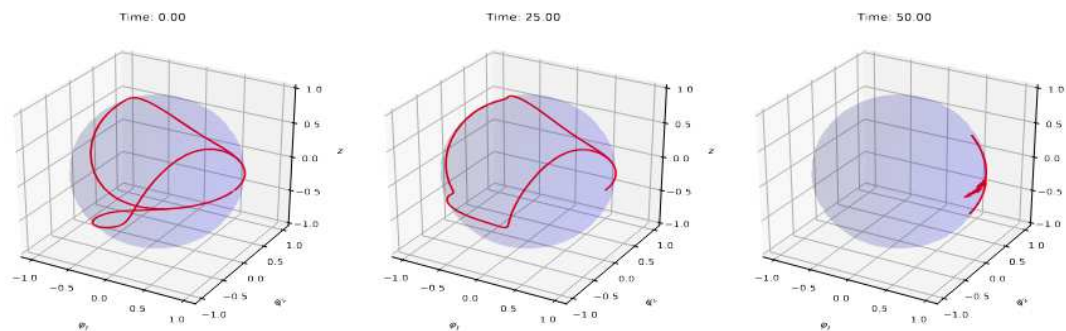
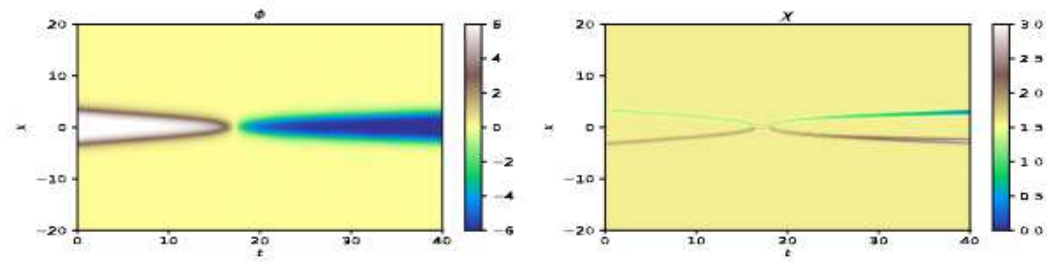
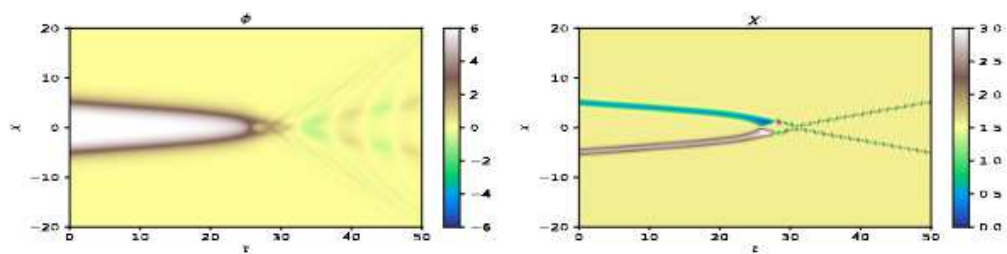
$$\begin{aligned}\chi(x, 0, x_0, v) &= \chi_L(\gamma(x + x_0 - vt)) + \chi_{\bar{L}}(\gamma(x - x_0 + vt)) + \frac{\pi}{2}, \\ \dot{\chi}(x, 0, x_0, v) &= \dot{\chi}_L(\gamma(x + x_0 - vt)) + \dot{\chi}_{\bar{L}}(\gamma(x - x_0 + vt)),\end{aligned}$$

$$\begin{aligned}\phi(x, 0, x_0, v) &= \phi_K(\gamma(x + x_0 - vt)) + \phi_{\bar{K}}(\gamma(x - x_0 + vt)) - 2\pi, \\ \dot{\phi}(x, 0, x_0, v) &= \dot{\phi}_K(\gamma(x + x_0 - vt)) + \dot{\phi}_{\bar{K}}(\gamma(x - x_0 + vt)),\end{aligned}$$

Kink-antikink and lump-antilump scattering

$v = 0.10, C = 0.5$

$v = 0.20, C = 3$



Conclusion

- The loops can develop interconnections in a complex pattern.
- We did not observe the production of separated loops.
- The numerical solution for kink-antikink and lump-lump scattering for small C suffer from numerical instability. This is shown to be the result of instability for $\chi = 0$.
- the limit $|C| \rightarrow \infty$ corresponds to the sine-Gordon solution for φ , with $\chi = \pi/2$. In this limit it is expected the scattering between the defects to be elastic, as occurs with the integrable (1, 1) sine-Gordon model
- our numerical investigation show how a nonintegrable defect constructed with two fields behaves due to scattering as one approaches the conditions for integrability.